

Road Surface Condition Detection with Machine Learning using New York State Department of Transportation Camera Images and Weather Forecast Data

Carly Sutter^{1,2,*} ORCID: 0009-0008-1414-4386

Kara J. Sulia^{1,*} ORCID: 0000-0002-4054-4956

Nick P. Bassill^{1,3} ORCID: 0000-0002-9105-0761

Christopher D. Wirz⁴ ORCID: 0000-0002-8990-5505

Christopher D. Thorncroft¹ ORCID: 0000-0001-7872-6459

Jay C. Rothenberger⁵ ORCID: 0009-0007-2530-4667

Vanessa Przybylo¹ ORCID: 0000-0003-4380-3543

Mariana G. Cains⁴ ORCID: 0000-0002-6729-6729

Jacob Radford⁶ ORCID: 0000-0001-6824-8967

David Aaron Evans^{1,2} ORCID: 0009-0003-1537-4996

¹Atmospheric Sciences Research Center, University at Albany, Albany, NY 12222, USA

²Department of Atmospheric and Environmental Sciences, University at Albany, Albany, NY 12222, USA

³State Weather Risk Communication Center, Albany, NY 12222, USA

⁴National Science Foundation National Center for Atmospheric Research, Boulder, CO 80305, USA

⁵School of Computer Science, The University of Oklahoma, Norman, OK 73019, USA

⁶Cooperative Institute for Research in the Atmosphere, Fort Collins, CO 80521, USA

* Corresponding authors: Carly Sutter (csutter@albany.edu), Kara J. Sulia (ksulia@albany.edu)

Abstract

The New York State Department of Transportation (NYSDOT) has a network of roadside traffic cameras that are used by both the NYSDOT and the public to observe road conditions. The NYSDOT evaluates road conditions by driving on roads and observing live cameras, tasks which are labor-intensive but necessary for making critical operational decisions during winter weather events. However, machine learning models can provide additional support for the NYSDOT by automatically classifying current road conditions across the state. In this study, convolutional neural networks and random forests are trained on camera images and weather data to predict road surface conditions. Models are trained on a hand-labeled dataset of $\sim 22,000$ camera images, each classified by human labelers into one of six road surface conditions: severe snow, snow, wet, dry, poor visibility, or obstructed. Model generalizability is prioritized to meet the operational needs of the NYSDOT decision makers, and the weather-related road surface condition model in this study achieves an accuracy of 81.5% on completely *unseen* cameras.

Keywords

- Winter weather
- Co-design
- Artificial intelligence
- Risk communication
- Hand-labeled dataset

Highlights

- Developed a model to classify road surface conditions using image and weather data
- Achieved accuracy of 81.5% on completely unseen cameras for weather-related classes
- Integrated co-design with end-users and interdisciplinary collaboration
- Designed methods that prioritize model generalizability for operational applicability

1. Introduction

Inclement weather affects traveler safety, with dangerous weather conditions leading to more than 1 million accidents in the U.S. each year (Anderson, 2024). Awareness of road surface conditions is essential for transportation agencies to know where resources (e.g., snowplows, treatments) are needed. The New York State Department of Transportation (NYSDOT) has a network of approximately 2400 live traffic cameras across New York state (NYS), which are situated at varying heights and pointing toward the roadways. These cameras (referred to as “sites” in this study) are publicly available at 511ny.org (NYSDOT, 2025) and winter road conditions are populated by the NYSDOT and displayed on a color-coded map (Fig. 1, left). Currently, the NYSDOT relies on manually observing individual cameras and driving on roads to determine the road surface conditions, both of which are time intensive. However, machine learning (ML) models, such as convolutional neural networks (CNNs) and random forests (RFs), can be used to automate the task of road surface condition classification. Compared to manual methods, the benefit of using ML is that predictions are made frequently (e.g., every five minutes) and at the individual camera level, which provides a granular spatial breakdown. When direct observation is not available, the integration of ML could enable more efficient and effective decision making because the model could automatically identify areas where roads are snow-covered and quickly accumulating (Fig. 1, right). The goal of this work is to use ML to make skillful predictions of road surface conditions on *unseen* camera sites (those not used in model training), prioritizing the operational needs of the NYSDOT.

Weather and road surface conditions have been shown to impact driver habits (Liu et al., 2025), affect traffic and accidents (Park et al., 2024), and therefore, affect traveler safety. The Federal Highway Administration (FHA, 2023) reported that over a 10-year period (2007 to 2016), 21% percent of vehicle crashes were weather-related. Of those weather-related crashes, 70% were due to wet pavement and 16% were due to snowy/slushy pavement. With high snow rates in NYS, the impacts were even greater. From 2010 to 2019, about 35% to 50% of crashes along the NYS Thruway in the month of January were associated with inclement weather, especially snowfall (Call and Flynt, 2022). Although fog was less frequent and accounted for only 3% of weather-related crashes in the US, it accounted for 9% of weather-related fatalities (FHA, 2023), indicating the importance of recognizing poor visibility conditions. These statistics emphasize the impact of road surface conditions on driver safety, motivating the work completed in this study.

1.1. Literature review

Research aimed at predicting road conditions from camera images has been completed using a variety of datasets and methods. Many earlier studies (Yamada et al., 2001; Kawai et al., 2014; Zhang et al., 2012; Sun and Jia, 2013; Yang et al., 2014; Lee et al., 2016; Kawarabuki and Onoguchi, 2014) employ methods of

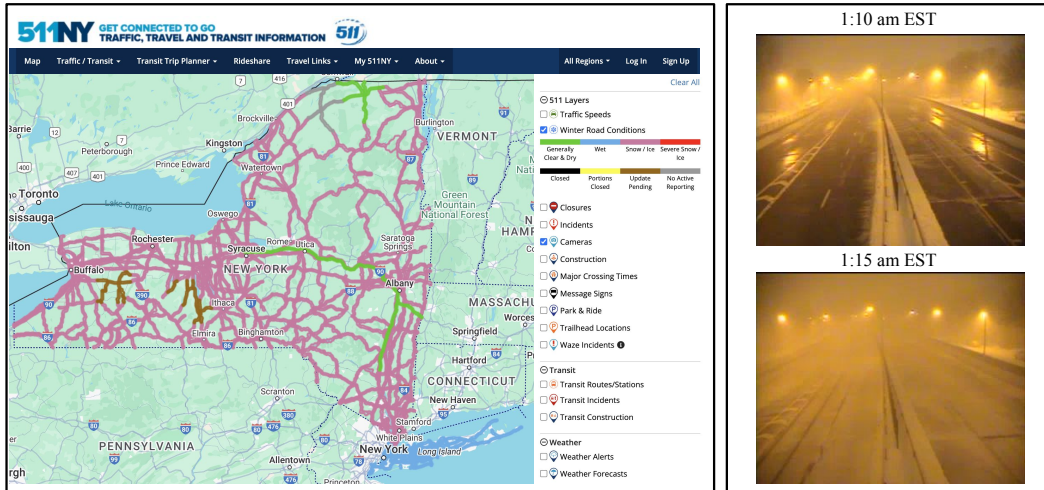


Fig. 1: Existing tool and motivation. (Left) Example of the 511ny.org map on February 6, 2025. Road surface conditions are color coded according to the key provided, with most of the state showing Snow/Ice conditions (pink). (Right) Example of one camera in Buffalo, NY on November 19, 2022, with two images taken five minutes apart, demonstrating how quickly snow can accumulate on the roads.

extracting features from images such as texture, edges, or hue, saturation, and value, followed by classification algorithms including K-nearest neighbors, Naïve Bayes, and Neural Networks to predict various road surface conditions, achieving accuracies ranging 87%-96%. A number of studies, including Yan et al. (2009), Omer and Fu (2010), Qian et al. (2016), Pan et al. (2018), Wu and Kwon (2022), use in-vehicle dash cameras from cars, buses, or snow plows to predict weather and road conditions. Various algorithms are used, such as Support Vector Machines and CNNs, achieving accuracies ranging 79%-93%. Other related studies incorporate information beyond road surface conditions, for example, Huang et al. (2024) use algorithms such as MonoDepth and XGBoost to predict different types of fog from roadway video data, Zhang et al. (2022) use CNNs to detect pavement distress like cracks and potholes, and Sirirattanapol et al. (2019) use multi-class CNN to predict multiple attributes including traffic levels, lighting, raining, and wet/dry road conditions. Road Weather Information System (RWIS) sensor data and camera images are used in Jonsson (2011) and Carrillo et al. (2020) to predict road surface conditions such as wet, dry, icy, and various levels of snow coverage, both works achieving accuracies above 90%. Differences in underlying datasets, classes, and applications hinder direct comparison between these past studies, however, they demonstrate that automatic road surface condition detection has been a consistent and important problem over time.

Past studies that are most similar to the work presented in this paper include Chang and Walker (2022), Carrillo and Crowley (2020), and Khan and Ahmed

(2022). Specifically, Chang and Walker (2022) used a dataset of 1000 NYSDOT images to predict “snow” or “no snow” conditions using Google’s Teachable Machine (Google, 2024), achieving test accuracy of 75% for the “snow” class and 95% for the “no snow” class. They also correlated image conditions with crash reports, finding that the chance of a crash increased by 61% when “snow” was predicted by the classification model. Carrillo and Crowley (2020) discussed drawbacks to using RWIS data, including their cost, which limits the number of RWIS sites, and suggests incorporation of the Ministry of Transportation of Ontario cameras as an important research consideration. Khan and Ahmed (2022) used roadside images from Wyoming DOT CCTV cameras to predict road surface conditions. Khan and Ahmed (2022) also discussed the benefits of using already-available DOT images, stating that they are more prevalent and readily available than RWIS sites given that webcams are more cost effective. They hand-labeled their image dataset with a weather condition (clear, heavy snow, and light snow) and a road surface condition (dry, snowy, and wet/slushy), and then built a separate classification model for each, achieving at least 97% validation accuracy on both. Khan and Ahmed (2022) also recognized the importance of testing their model on other roadways, so they tested their model on a small subset of 300 completely new cameras, achieving a high accuracy of 95.3%. Their work does not include poor visibility or obstruction, and the importance of these classes are included in Section 2; more comparisons to Khan and Ahmed (2022) and the work presented in this study are discussed in Section 4.1.

1.2. Contributions

This study focuses on methods that are important for building a trustworthy model (Bostrom et al., 2023) with the NYSDOT that can also be applied to broad range of scenarios and other locations. Many past studies sought to solve a similar task of automating road weather condition classification; however, some limitations of past studies include the use of one or few camera sites, the use of a limited number of road surface classes, omission of details about the underlying datasets and labeling techniques, evaluation on images from the same camera, or reliance on other equipment like in-vehicle dash cameras or expensive sensor data. Relative to past studies, five main contributions of the work presented in this paper include:

1. Close collaboration with the NYSDOT with the goal of creating a model that is trustworthy, a concept referred to as “co-design” (Bostrom et al., 2023).
2. Dataset curation integrates social science techniques and risk communication perspectives, ensuring transparent rules for human labeling that enhance understanding and can be applied to new camera systems.
3. Emphasis on improving model performance on *completely new* camera sites. Generalizability is a critical aspect to consider in order to eventually operationalize use of the model by the NYSDOT and other transportation agencies.

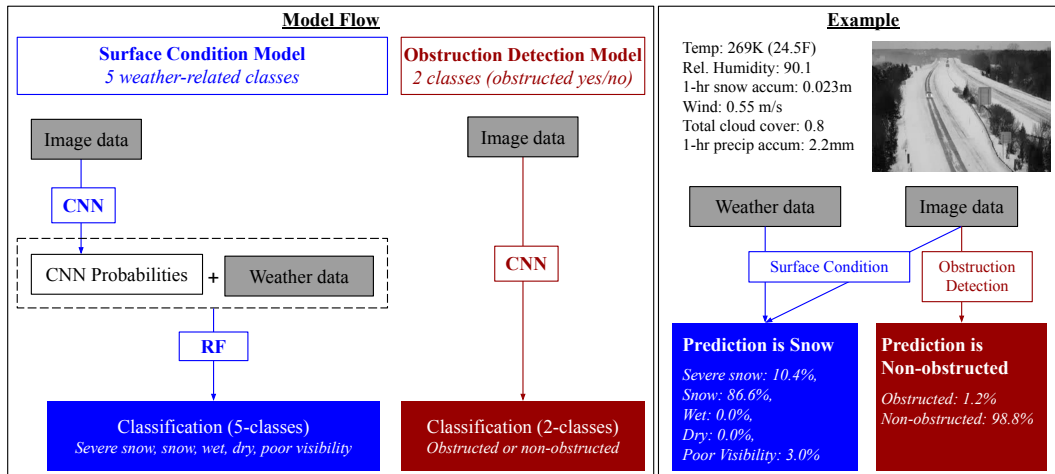


Fig. 2: Operational model flow and example. (Left) The Surface Condition Model is a two-stage process using a CNN and a RF. The Obstruction Detection Model solely predicts whether an image is obstructed of non-obstructed. (Right) The model flow in a practical inference scenario is shown, demonstrating that both predictions will be provided in conjunction for each new observation.

4. Creation of a robust dataset containing 45 unique cameras sites of *varying quality* that are representative of cameras across the state, rather than including only high quality images that inflate performance.
5. Inclusion of varied classes that encompass a wide range of road surface conditions that are prevalent in images and critical for operational needs, developed in collaboration with NYSDOT.

1.3. Overview

Six road surface condition classes (severe snow, snow, wet, dry, poor visibility, and obstructed) are predicted from camera images and weather data using supervised ML models. Figure 2 shows the general flow of the modeling process: a Surface Condition Model that predicts weather-related classes using a CNN model and a downstream RF model, and an Obstruction Detection Model that uses a CNN. Section 2 discusses the datasets used in this work, including a hand-labeled image dataset and High-Resolution Rapid Refresh (HRRR) weather forecast data. Section 3 includes details on training and selecting ML models. Model performance and generalizability are discussed in Section 4. The terms “prediction” and “predict” are used to refer to a model’s classification output. A primary focus of this work is to understand how the model performs on unseen camera sites, referred to as “generalizability”. Generalizability is critical for meeting operational needs that involve deploying the road surface classification models on thousands of cameras across NYS.

2. Data

2.1. Image and Weather Data

Camera images are utilized to create a labeled dataset, which serves as the foundation for developing ML models in this study. Images are viewed manually by human labelers who assign a road surface condition classification to each image. A systematic approach from social science, known as Quantitative Content Analysis (Coe and Scacco, 2017), is used to label the images in this study. This approach includes the development of a codebook, which serves as thorough documentation of classification rules and definitions to ensure replicability and reproducibility, as published in Wirz et al. (2024). The New York State Mesonet (NYSM; Brotzge et al., 2020) observational weather data are used to aid in hand-labeling. Comprehensive documentation for the data used in this study is available at Sutter et al. (2025b); a total of 21,653 images from 45 unique camera sites across NYS are labeled for this study. Table 1 shows examples of the six labeled classes, and detailed definitions for each class are provided in the codebook from Sutter et al. (2025a).

A large focus of this work is to create a model that performs well on a wide range of conditions that are realistically encountered in the installed cameras. For example, the obstructed cases seem less important because they are generally not weather related, but nonetheless, they are included because they are observed frequently and can deem the observation as unreliable. Similarly, cameras that are of lower quality but are not obstructed (right-hand side of Table 1) are included in this study. While past studies may have included difficult examples like these, they have not been emphasized, and the focus of this work is to provide a model that can work on representative images from already-implemented cameras, which include these less-than-ideal cases. Building one model that can predict road surface conditions across a wide range of conditions on all cameras (including low quality cameras), creates a tool that is operationally realistic for the NYSDOT.

The High-Resolution Rapid Refresh (HRRR, 2024) is a weather forecast model providing information like forecasted snowfall, rainfall, temperature, and wind speeds. HRRR forecast data are updated hourly and used in a wide range of applications where weather predictions are needed (Alexander et al., 2013). The labeled image data and forecast data are collated based on time and location resulting in corresponding forecast data for each labeled image. The forecast data being used is forecast hour two, with valid time corresponding to the time of the paired labeled image. The HRRR data are used in favor of observational data because of its fine spatial grid of 3km. The average distance from each camera to the nearest HRRR grid point is 1.1km. Six HRRR weather forecast variables are used in this study, including 2-meter temperature, 2-meter relative humidity, 10-meter average wind speed, 2-hr accumulated snow depth, 2-hr total precipitation, and total cloud cover, but other HRRR data variables should be considered in future work. Since five of the labeled classes in this study are weather-related, it is reasonable to include weather

Table 1

The six road surface conditions are shown with examples and count distribution, totaling to 21,653 images. The right-most column shows examples of high- and low-quality images. The high-quality image is well lit even in the absence of car headlights, making the classification of road surface conditions more obvious. The low-quality image is poorly lit and is distanced far from the roadway, making the classification of these images more difficult; in these cases, the labeler relies on slight changes in road pavement darkness as well as NYSM observational data (Sutter et al., 2025a).

Six classes			Site Quality
Severe snow - 1,527 	Snow - 2,989 	Wet - 8,458 	High Quality - 58% 
Dry - 7,600 	Poor visibility - 915 	Obstructed - 164 	Low Quality - 42% 

data in the modeling process for the Surface Condition Model, and doing so made a positive impact to model performance, as discussed in Section 4.3. The obstructed class is generally not weather-related, so HRRR data are not used for the Obstruction Detection Model (see Fig. 2).

2.2. Data splitting

The data is split to ensure that model evaluation aligns with the goal of generalizability. Specifically, a “site-specific” split method is used where all observations from a site are in the same fold, which ensures that training, validation, and testing contain unique sites.

Nested cross-validation (CV) is used for the Surface Condition Model to ensure that each stage of the modeling process is evaluated on data not used in model training. The labeled data is split into six folds of approximately equal size (16.67%) that serve as the training data, validation data, or testing data at different points in the modeling process. Training dataset 1 is used to train the CNN, and training dataset 2 is used to train the RF model; the benefit of using separate datasets are discussed in Sections 3.2.2 and 4.3. Additionally, the nested structure allows for a more robust evaluation of ensemble methods (compared to a single test set) because each fold serves as the test dataset (see Section 3.4). Data splitting is demonstrated visually in Fig. 3.

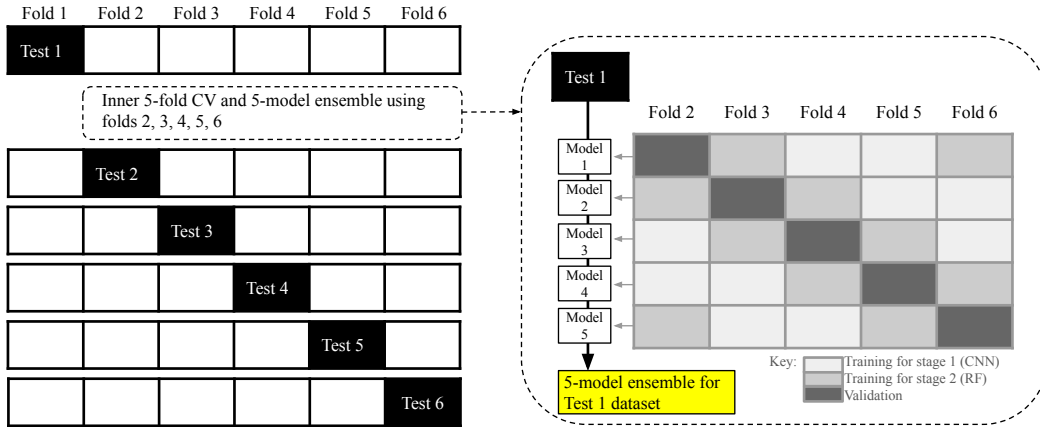


Fig. 3: Nested CV for the Surface Condition Model. For each test dataset (black cells), inner 5-fold CV is used on the remaining five folds (right), resulting in five models. The five models are used to create an ensemble prediction for the test dataset. This process is demonstrated for Test 1 and is repeated for each test set (left).

For the Obstruction Detection Model, there are only 164 examples of obstructed images. Three sets of non-obstructed images are sampled from the 5-class dataset, and undersampling is done purposefully to be approximately equal to the number of obstructed samples, while also representing observations from each class and site from the 5-class dataset, resulting in 194 non-obstructed images. In total, the two-class dataset for the Obstruction Detection Model contains only 358 images, and two-fold CV is used due to the limited number of observations. Two-fold CV provides the training and validation datasets only. Generally, it is not a best practice to omit a testing dataset, however, for the Obstruction Detection Model, the validation data is only used so much as to stop model training before overfitting occurs; no model testing or hyperparameter tuning is done (see Sections 3.2.3 and 3.3). Thus, using two-fold CV provides a practical solution given the limited size of the dataset. The purpose of three different samples of non-obstructed images is to provide a framework for ensembling. Although the obstructed examples are the same between each of the three datasets, having different non-obstructed examples makes for three different datasets that are trained separately and used to create a 3-member ensemble. This approach provides a way of doing ensembling without nested CV, which is impractical with this small dataset. Data splitting for the Obstruction Detection is shown in Fig. 4.

3. Modeling methods

The labeled dataset and its corresponding image and weather data are used to predict road surface conditions across NYS. Classification ML algorithms, including CNNs and RFs, are trained to categorize each observation into one of five road surface classes for the Surface Condition Model. For the Obstruction Detection Model, a

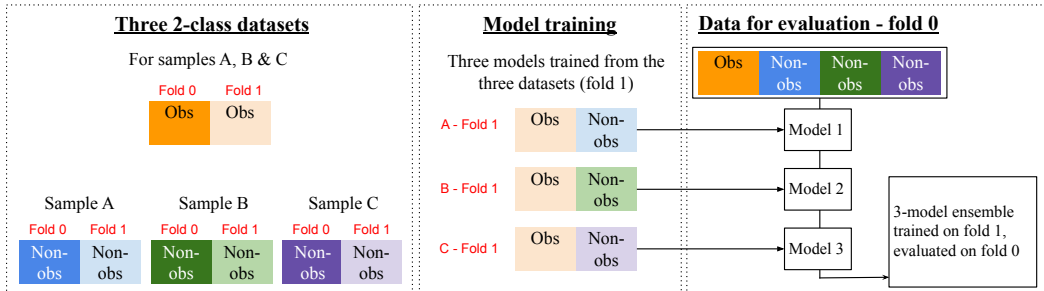


Fig. 4: Data splitting for the Obstruction Detection Model. Sampling, 2-fold CV, and ensembling for the two-class dataset is shown.

CNN is utilized to classify each observation as either obstructed or non-obstructed. Lastly, ensembling methods are employed to utilize the predictions from multiple models trained on different datasets, as discussed in Section 2.2. For all ML methods in this section, input data are subject to relevant normalization or preprocessing prior to training. Balanced class weighting is used to address the imbalanced dataset (Table 1), which is important to encourage the model to learn all classes rather than simply learning to predict majority classes, like wet and dry.

3.1. Image classification

Images contain a wide range of colors, textures, edges, and nonlinear, complex patterns. CNNs are commonly used image models because they can automatically extract these complex features in images to learn a classification task. Spatial relationships that exist in the images are learned through filters and convolutional layers (Chase et al., 2023), and nonlinearity in the data is learned by filters and convolutional layers with activation functions. Many different CNN models are trained to identify the best performing architectures and hyperparameters for this task.

The CNN models are trained on NVIDIA A100 and V100 GPUs using the Tensorflow python package (TensorFlow Developers, 2024). Images are cropped to remove the top 20% of the image that often contains text (e.g., timestamps or location, examples in Table 1) or is not focused on roadways (e.g., sky or distant scenery). Images are resized to 224x224 and encoded as RGB. Cropping, resizing, and standardization of the data are preprocessing steps that are done on the fly during data loading. The model weights from the epoch achieving highest validation accuracy are saved as the product of training. Table 2 shows additional CNN modeling details.

3.2. Surface Condition Model methods

3.2.1. CNN models and hyperparameter tuning

For the Surface Condition Model, a set of 36 baseline CNN models are trained to identify the best performers, of which the best four (according to the criteria listed in Section 3.2.3) are selected for further hyperparameter tuning. The 36 baseline models

Table 2

Training configuration summary for CNN models. Learning rate is indicated as LR.

Loss	Optimizer	Init. LR	Momentum	LR Decay	Batch Size	Epochs	Early Stopping
Categorical Cross-Entropy	Stochastic Gradient Descent	0.01	0.25	Exponential (0.95)	128	30–75	Val acc. incr. < 0.5% in 10 epochs

are comprised of a combination of six different architectures, three different uses of transfer learning, and the presence or absence of data augmentation.

Six CNN architectures, which range in complexity, include DenseNet121 from Huang et al. (2016), InceptionV3 from Szegedy et al. (2014), Mobilenet from Howard et al. (2017), ResNet50 from He et al. (2015), VGG16 from Simonyan and Zisserman (2015), and Xception from Chollet (2017). Data augmentation is used to diversify the training set by applying transformations to the original images. Such transformations include adjusting the brightness and/or contrast in the image, and horizontally flipping the image. These augmentations are made automatically and randomly to images on the fly during model training, with replacement, to make the dataset more robust and varied (TensorFlow Developers, 2024).

Transfer learning involves using pretrained models where the backbone of the architecture (which include convolutional layers) is frozen; the weights are already learned from the commonly used ImageNet dataset (Deng et al., 2009). The Keras library provides both the architectures and pre-trained weights that are used for this work (Chollet and et al., 2015). The final layers of the architecture are the dense layers that ultimately result in the final classification, and will be referred to as the “top” of the model. The top is always trained specifically on the NYSDOT dataset. Two different architecture tops are considered: 1) the generic top (referred to as “GEN”) consists of a 2D global average pooling layer followed by three dense layers of size 1024, 512, and six (the output layer), and 2) the architecture-specific top (referred to as “AST”) consists of layers that align with the original architecture. The third consideration is the exclusion of transfer learning meaning that all weights from all model layers are trained using the NYSDOT dataset. Thus, the use of transfer learning with two different tops (GEN or AST), as well as the exclusion of any transfer learning, comprise three choices related to transfer learning that are considered in the baseline search.

For hyperparameter tuning, L2 regularization and dropout are common regularization techniques used to reduce overfitting in CNN models (Géron, 2020). These regularization techniques are used on the top dense layers, and hyperparameter tuning is completed to identify the best performing L2 regularization weight and dropout rate. For the baseline models, these hyperparameters are set to 0. The hyperparameter space, shown in Table 3, includes four different L2 regularization weights ranging

Table 3

CNN model considerations. Baseline models are run (36 combinations), and then the top baseline models undergo hyperparameter tuning. **The red text indicates the final best CNN model** that is chosen and discussed in Section 4.1.

Baseline model choices			Hyperparameters	
Architecture	Transfer Learning	Augment.	Dropout	L2
Densenet, Inception, Mobilenet, Resnet , VGG16, Xception	None Transfer Learn: AST Transfer Learn: GEN	Aug. No Aug.	0.0, 0.2 , 0.4, 0.6, 0.8	0.0, 1E-7, 1E-5, 0.001, 0.1

from 0.2 to 0.8, and four dropout rates ranging from 1E-7 to 0.1, resulting in 16 sets. Thus, including the baseline runs, there are 17 hyperparameter sets tested in total.

The modeling process begins with running the 36 baseline models, from which the top four are selected using the model selection criteria discussed in Section 3.2.3. The four models then undergo hyperparameter tuning, and one top performing hyperparameter set is selected for each. Thus, four final CNN models for image classification are considered and carried over into the next step of the modeling process, the downstream classification ML model, which incorporates information from the CNN as well as weather data, as discussed in the next section. The final CNN is selected following hyperparameter tuning of the downstream model.

3.2.2. Downstream random forest classification with weather data

The Surface Condition Model is a two-stage approach that begins with image classification (CNN) and is followed by downstream classification model, a random forest (RF) trained on both weather data and the probability output of the CNN model. The RF model is considered “downstream” because it requires the output from the CNN, and also because it is trained on a separate dataset (training dataset 2) that is *not* used to train the CNN models, as shown in Fig. 3. This downstream RF model serves two purposes. First, it incorporates weather data into the modeling process, which is relevant given that the five classes are weather related. Second, by training the model on unseen observations (using training dataset 2), the RF model is able to adjust for biases in the CNN by learning when the CNN predictions are more (or less) correct and refine its prediction by considering the weather. Improvements gained from adding weather data are discussed in Section 4.1 and shown in Fig. 6.

First, the CNN model from stage 1 is used to generate predictions (inference) on training dataset 2. Probabilities are normalized to sum to one after calibrating the predicted class using isotonic regression, a common technique used to create better alignment between predicted probability and accuracy (Pedregosa et al., 2011; Jiang et al., 2011; Hollance, 2022). Next, the weather data are collected for the time and location corresponding to each image in the hand-labeled dataset (Section 2). The five probabilities and the six weather variables comprise the 11 inputs for

Table 4

Surface Condition Model - Downstream Model Tuning. Algorithms including dense neural network (DNN), Gaussian Naive Bayes (GNB), Support Vector Machines (SVM), and Random Forest (RF), and corresponding hyperparameters, are tested. The **red text indicates the final selected model** (discussed in Section 4.1).

Algorithm	Hyperparameters
DNN	Hidden layer nodes: [256,128,64,32,16], [128,64,32,16], [64,32,16], [32,16], [16] Dropout: 0, 0.2, 0.4, 0.6, 0.8 L2: 0, 0.001, 0.01, 0.1
GNB	var_smoothing: 1e-12, 1e-11, 1e-10, 1e-8, 1e-7, 1e-6
Logistic	max_iter: 100, 300, 500 C: 0.01, 0.1, 1.0, 10.0, 100.0
SVM	C: 1e-3, 1e-2, 0.1, 1, 10, 100 gamma: 1e-7, 1e-5, 1e-4, 1e-3, 1e-2, 0.1, 1, 10
RF	n_estimators: 25, 100, 300 max_depth: 5, 10 , 20, None max_features: 3 , 6, 10 min_samples_leaf: 1, 5 bootstrap: FALSE, TRUE max_samples: 0.5 , 0.75, 1

the RF model, and the hand-labeled classification is the target variable. A random forest is selected for this stage in the modeling process, but other algorithms and hyperparameter combinations are tested, as shown in Table 4. The hyperparameters affect the complexity of each algorithm, thus affecting model performance.

A random forest is a commonly used ML algorithm that captures nonlinear relationships in data (Auret and Aldrich, 2012). It is an ensemble of decision trees where each tree makes a sequence of decisions and ultimately places each observation into a final leaf node. The gini impurity index is used as the loss function (Géron, 2020) to train the model. The python ML package, scikit-learn (Pedregosa et al., 2011), is used to train RFs for this task. The outputs of the RF are model predicted classes and the probabilities of each class. A random forest is selected as the best performing model (Section 3.2.3), but another benefit of utilizing RFs is that feature importance can easily be implemented. Feature importance provides information about the contribution of each input variable, which can be helpful for determining which variables to include in model training, as well as for understanding which features the model relies heavily on to make its classification (see Section 4.3).

3.2.3. Model selection

Three parts of the modeling process require model selection: (A) selecting the top four baseline models for hyperparameter tuning, (B) selecting the top hyperparameter-tuned models that are then used in the downstream model, and (C) selecting the final model. All models are evaluated on validation data using the nested-CV setup (Fig. 3); there are six test datasets with 5-fold CV, totaling 30 different datasets used

for training and evaluating each ML model. Results are aggregated across the 30 validation datasets, and model selection is performed by considering multiple metrics that align with the goals of this work while also accounting for intricacies of the imbalanced dataset, as discussed below.

Accuracy is the percentage of correct model predictions (number of correct predictions divided by the number of total observations), and recall can be thought of as a measurement of accuracy *within* a given labeled class (e.g., number of correct snow predictions divided by the number of observations labeled snow). Recall, precision, and F1 score are metrics that are commonly used in ML (Géron, 2020), but in this study, recall is prioritized because it is the class-specific metric that minimizes the number of misses, which is especially important for this work. As an example, it is crucial for traveler safety that the model does not miss severe snow cases, and recall is the metric that captures this goal. Additionally, since recall measures the performance relative to the number of labeled images in each class, it is an appropriate metric to use with the largely imbalanced dataset. Relying on accuracy alone is insufficient because it is heavily influenced by class imbalance. Performance of *each class* is important for this application, and this is accounted for by calculating the average recall across the five classes (i.e., an average of the five metrics: severe snow recall, snow recall, wet recall, dry recall, poor visibility recall). This average recall metric serves as a more *balanced* performance metric because each class has an equal contribution, rather than accuracy, which is heavily skewed toward the majority classes. Both metrics - accuracy and average recall - are calculated on the validation data and used for model selection by *first* narrowing to the top-performing models based on average recall, and then selecting the model with the highest accuracy among them.

3.3. Obstruction Detection Model methods

For the Obstruction Detection Model, only a CNN is used because the task is strictly image classification: obstructed or non-obstructed. As discussed in Section 2.2, this model has limitations due to the small dataset with only 164 obstructed examples. With two-fold CV, there is only one validation dataset (no testing dataset), which is needed for model evaluation. Any extensive hyperparameter tuning would *also* require the use of the validation dataset for model selection, which can skew model evaluation results that use the same validation data. Given these limitations, the final CNN architecture and hyperparameters selected for the Surface Condition Model are used to train the Obstruction Detection Model.

3.4. Ensembling

The data used in this work is variable given the inclusion of many camera sites with varying backgrounds, lighting, and distances from the road. Using one holdout test dataset could lead to performance metrics that do not realistically represent performance if the sites are not perfectly representative of the overall dataset. Thus, for the Surface Detection Model, six distinct test datasets are used, and each one uses

5-fold CV, for which the five models comprise the model ensemble for the outside test dataset, as shown in Fig. 3. Ensembling combines the outputs from each of the five models to produce one final prediction. Ensembling is chosen for this application because it can be useful in operations to provide a measure of confidence. Three methods of ensembling are used: (1) average class probabilities, (2) majority vote, and (3) highest-confidence prediction (with calibrated probabilities). Method 1 is used as the prediction when it agrees with either method 2 or 3, otherwise method 2 is used when the prediction agrees with method 3, and lastly, if none agree, the most severe weather condition prediction is used. The same procedure is applied to the obstruction detection model, using a 3-member ensemble (Fig. 4).

4. Results and discussion

This section includes results for the Surface Condition Model and the Obstruction Detection Model, and it ends with a discussion on generalizability, which is an aspect of this work that is critical for the application to NYSDOT.

4.1. Surface Condition Model results

For the CNN model, there is a 19-percentage point validation accuracy difference between the best and worst baseline models. Densenet, Mobilenet, and Resnet are generally top performing architectures, but the overall performance also depends on the choices of augmentation and transfer learning, as shown in Fig. 5A. Ultimately, the final CNN from model selection (Section 3.2.3) is a Resnet architecture, using transfer learning with the architecture-specific top (AST), augmentation, dropout rate of 0.2, and L2 regularization rate of 0.1. Hyperparameter tuning and the selection of dropout rate and L2 regularization provide a boost of approximately one percentage point. The selected CNN achieves a validation accuracy of 69.1%.

For the stage 2 downstream model that incorporates weather data, five classification algorithms with varying hyperparameters are tested (see Section 3.2.2 for details). The top performing architecture for each algorithm is shown in Fig. 5B. The GNB model has the lowest performance, while the DNN, RF, and SVM algorithms all have accuracies and average recall greater than 75%. The final selected algorithm is an RF of 300 decision trees with a max depth of 10, a maximum of three features considered in each split, a minimum of five samples per leaf node, and bootstrap sampling of 0.50. This model achieves validation accuracy of 80.7%.

The last step in the Surface Condition Model is to get a final prediction for the test dataset by ensembling across the five models (see Fig. 3 and Section 3.4). Figure 6 shows the test accuracy for every step in the modeling process. Incorporating weather data with the RF provides a significant increase in performance, as shown by the accuracy gain of +12.1 percentage points from stage 1 (68.1%) to stage 2 (80.2%). Ensembling provides an additional +1.3% accuracy increase, resulting in a **final test accuracy of 81.5%**. Given the small performance improvement gained from ensembling, deployment of future operational models should consider

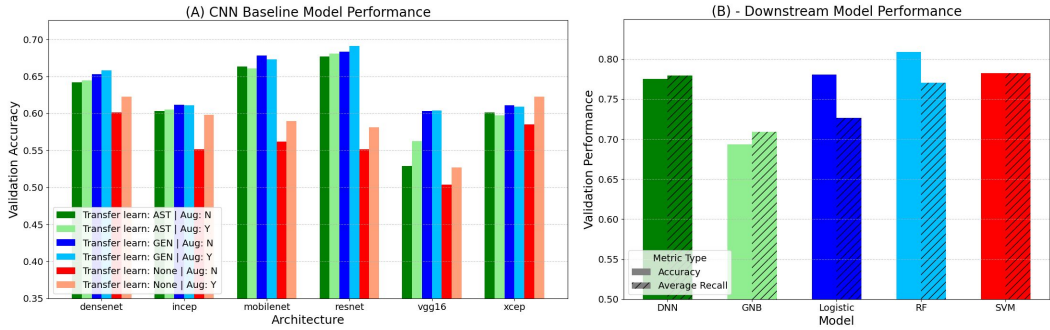


Fig. 5: Surface Condition Model: Validation Performance Comparison Across Models. (A) Validation accuracy of the 36 baseline CNN models are shown; this includes Architecture-Specific Top (greens), Generic Top (blues), and None (reds), and the inclusion of Augmentation (lighter shades), and No Augmentation (darker shades). (B) The top performing hyperparameter set for each of the five algorithms from the stage 2 downstream model are shown, including overall accuracy, as well as average recall metric.

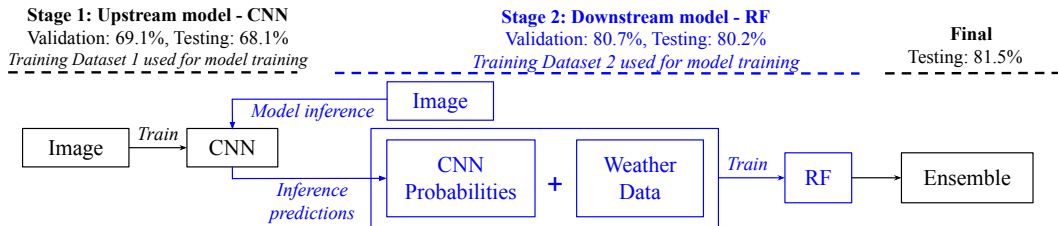


Fig. 6: Net Gain in Performance by Step for the Surface Condition Model. Accuracy on the test dataset is shown for every stage in the modeling process.

whether the performance improvement is worth the computational cost associated with ensembling, which creates five times as many models.

The final model improves predictions compared to the CNN alone, and the most significant improvements are in the snow and dry classes, which increase by 17.3 and 24.3 percentage points, respectively, as shown in Table 5. For the final model, the classes with the lowest recall are wet, poor visibility, and snow, and this is a reasonable result given that these classes border multiple classes. For example, a simplified progression of a winter weather event is: dry \leftrightarrow wet \leftrightarrow snow \leftrightarrow severe snow. Snow and wet appear in the middle as “transitional” phases, and therefore have more opportunity for misclassifications, as shown in Table 5. Out of all of the model’s errors, 95.5% fell into one of the adjacent classes, which shows that the model makes reasonable errors that align with difficulties that humans also encounter when labeling observations. Similarly, poor visibility is a difficult class given that there are many conditions that can lead to this class, including dense fog, heavy snow, or heavy rain.

As a comparison, the results of Khan and Ahmed (2022) show a validation accuracy of 95.2% on a sample of 300 camera images from different sites, which

Table 5

Class recall metrics. Performance by class for the CNN and final model are shown.

Hand-labeled class	CNN Recall	Final Recall	Common misclassifications
Severe snow	77.2%	81.5%	Snow
Snow	59.8%	77.1%	Wet, severe snow
Wet	70.6%	75.9%	Dry, snow
Dry	65.8%	90.1%	Wet
Poor visibility	75.0%	76.8%	Wet, severe snow, dry

is higher than the results achieved in this work. This lower accuracy could be due to a variety of factors, including 1) lower camera quality in the NYSDOT images, 2) the inclusion of more road surface classes in the NYSDOT images (e.g. severe snow and poor visibility) and 3) testing on a larger dataset of approximately 3500 held-out images. The importance of data representation is discussed in detail in Section 4.3.

4.2. Obstruction Detection Model results

The overall performance for the obstructed class is 88.4% and for the non-obstructed class it is 97.8%. Operationally, both the Surface Condition Model and the Obstruction Detection Model could be beneficial to NYSDOT practitioners, thus, all observations would go through both models to provide predictions from each. Model inference of the Obstruction Detection Model on the entire 5-class dataset (21,653) shows that the model correctly predicts non-obstructed on 98.3% of the labeled 5-class observations, which is even higher than the subset of 194 sampled non-obstructed images that are used in validation (i.e., the 97.8% recall).

4.3. Generalizability takeaways

The choice to have two training datasets - training dataset 1 for the CNN, and training dataset 2 for the RF - inherently aligns with the goals of generalizability because it incorporates training from sites that are unseen from the CNN. The value in doing this is proven further by running an experiment where the RF and CNN are trained on the *same* dataset, using all four training folds from Fig. 3. The validation skill decreases 2.2% (from 80.7% to 78.5%), supporting the usefulness of training on a downstream model. Additionally, feature importance analysis is performed to explain the contribution of each input variable in terms of model skill. When the CNN and RF are trained using the same dataset, the contribution of weather data is only 21%, whereas the contribution is higher, 34%, when models are trained on separate datasets. This result supports the decision to train on separate datasets because it encourages more balanced contribution from weather and image data.

Another experiment is run to confirm the usefulness of incorporating weather data for generalizability. For this experiment, an alternative shuffle-split method is employed where each site is represented in every fold. This method has higher

validation accuracy, which is expected because the model is trained on every site that exists in validation, and is not applicable for the operational end goals of this work. With the shuffle split method, validation accuracy for stage 1 (CNN) is 80.8% and stage 2 (RF) is 86.8%, which is an accuracy increase of 6 percentage points. However, the site-specific split method has a validation accuracy increase of +11.6 percentage points (69.1% to 80.7%, as shown in Fig. 6), which is nearly double that of the shuffle split method. This comparison indicates that the incorporation of weather data downstream plays a critical role in improving model generalizability.

The importance of site representation is demonstrated with an additional experiment where half of the camera sites are removed from the labeled dataset. The same sites are removed from both the shuffle split and site-specific split, and the halved datasets contains the same proportion of both high-quality and low-quality sites compared to the full dataset. The purpose of conducting this experiment is to answer the question of whether more data, specifically more data from *more sites*, is helpful for generalizability. For the site-specific split method, results show that halving the dataset reduces model accuracy by approximately -3.2 percentage points (from 80.7% to 77.5%), while the shuffle split only has a reduction of approximately -0.1 percentage point (from 86.8% to 86.7%). This indicates that more data from new camera sites is particularly helpful for generalizability because the site-specific method sees a greater benefit from the inclusion of more sites. Furthermore, low quality sites (examples shown in Table 1) especially benefit from the addition of more sites with an accuracy increase of +6.4%, whereas high-quality sites see an increase of only +1.8%.

Overall, low quality sites perform worse than high-quality sites, with low-quality sites having validation accuracy of 74.1% and high quality with 85.5% (with overall validation accuracy of 80.7%). This means that a task may be made more difficult by the inclusion of low-quality sites. This performance contrast is intuitive, but it raises interesting considerations for dataset curation and model development. Site representation is critical given the goal for statewide deployment, but it is something that can easily be neglected due to the difficulty of labeling poor-quality sites, as well as lower performance metrics associated with lower quality sites. However, it is important to recognize that, in this context, lower accuracy does not necessarily mean it is a “worse” model because the end goal of this work is to develop a model that can be applied on cameras across NYS, and those cameras *do* range in quality. Deploying a model heedlessly without considering representation could result in an inapplicable operational model. End-users, data curators, and model developers must work together to ensure the application is being met.

5. Conclusions

The NYSDOT has a large network of camera images that are used to automatically classify road surface conditions. A systematic hand-labeling process known as

quantitative content analysis (QCA) is followed to create a well-documented hand-labeled dataset that is used as the target variable for training ML algorithms. The Surface Condition Model predicts severe snow, snow, wet, dry, or poor visibility using CNNs and RFs trained on camera images and weather data. The Obstruction Detection Model predicts obstructed or non-obstructed using camera images and a CNN. The test accuracy of the final Surface Condition Model is 81.5%, and the Object Detection Model detects obstructed observations with a recall of 88.4%.

Labeling images from every camera site is not feasible, nor does it provide a pathway for new states or regions to implement this model. Thus, the performance of unseen camera sites is prioritized in this study. One major takeaway is that the inclusion of weather data proves to be particularly beneficial for increasing model generalizability. Additional experiments reveal that more data, specifically from new and diverse sites, improve model generalizability, especially on low-quality cameras. Thus, adding more sites through additional labeling should be considered in the future and can be done reliably given the QCA process and documentation employed in this work. Another consideration for future work is that there are other ML techniques that perform well with limited data and these should also be explored, such as co-training or discriminative self-supervised learning (Rothenberger and Diochnos, 2024).

The inclusion of low-quality sites and difficult classes like poor visibility make the task more difficult but are important because the broader purpose of this work is to provide an automated product for the NYSDOT to use operationally. Collaboration with the NYSDOT is critical for the adoption and usability of this work. The models in this study can provide a helpful tool to monitor current road surface conditions because it can update frequently (every five minutes) and vastly (at the camera level), which is of value to the NYSDOT, and can be applicable to other states and regions. Resource allocation and driver safety are crucial, and with the range of winter weather conditions that New York State experiences, this study presents a method of automated road surface classification that can offer pertinent insights during hazardous events.

CRedit authorship contribution statement

Carly Sutter: Conceptualization, Data curation, Formal analysis, Investigation, Methodology, Software, Visualization, Writing – original draft. **Kara J. Sulia:** Conceptualization, Funding acquisition, Methodology, Resources, Supervision, Writing – review & editing. **Nick P. Bassill:** Conceptualization, Funding acquisition, Methodology, Resources, Supervision, Writing – review & editing. **Christopher D. Wirz:** Conceptualization, Data curation, Investigation, Methodology, Supervision, Writing – review & editing. **Christopher D. Thorncroft:** Conceptualization, Funding acquisition, Resources, Supervision, Writing – review & editing. **Jay C. Rothenberger:** Conceptualization, Investigation, Methodology, Writing – review & editing. **Vanessa Przybylo:** Conceptualization, Data curation, Investigation, Methodology, Writing –

review & editing. **Mariana G. Cains:** Data curation, Investigation, Methodology, Writing – review & editing. **Jacob Radford:** Data curation, Investigation, Writing – review & editing. **David Aaron Evans:** Data curation, Investigation, Writing – review & editing.

Data availability statement

The dataset is private, but comprehensive information is provided in Sutter et al. (2025b). The code is available at <https://github.com/cgsutter/DRIVE-clean>.

Declaration of competing interest

The authors have no known competing financial interests or personal relationships that could have appeared to influence the work reported in this paper.

Acknowledgments

This material is based upon work supported by the U.S. National Science Foundation under Grant No. RISE-2019758. This work is part of the NSF AI Institute for Research on Trustworthy AI in Weather, Climate, and Coastal Oceanography (NSF AI2ES). This research is also made possible by the New York State (NYS) Mesonet. Original funding for the NYS Mesonet (NYSM) buildup was provided by Federal Emergency Management Agency grant FEMA-4085-DR-NY. The continued operation and maintenance of the NYSM is supported by National Mesonet Program, University at Albany, Federal and private grants, and others. The xCITE lab (XCITE, 2025) provided computational resources for model development.

References

- Alexander, C., Benjamin, S., Dowell, D.C., Smirnova, T.G., James, E.P., Hofmann, P., Hu, M., Brown, J., 2013. The high-resolution rapid refresh (hrrr): Accessibility of next generation convective-scale forecast guidance from research to operations, in: 93rd American Meteorological Society Annual Meeting 2013, American Meteorological Society, Austin, Texas, USA. p. 4.5.
- Anderson, A., 2024. Predicting hazardous road conditions. National Center for Atmospheric Research. URL: <https://ral.ucar.edu/solutions/benefits/predicting-hazardous-road-conditions>. accessed 14 April 2024.
- Auret, L., Aldrich, C., 2012. Interpretation of nonlinear relationships between process variables by use of random forests. *Minerals Engineering* 35, 27–42. doi:10.1016/j.mineng.2012.05.008.
- Bostrom, A., Demuth, J.L., Wirz, C.D., Cains, M.G., Schumacher, A., Madlambayan, D., Bansal, A.S., Bearth, A., Chase, R., Crosman, K.M., Ebert-Uphoff, I., Gagne II, D.J., Guikema, S., Hoffman, R., Johnson, B.B., Kumler-Bonfanti, C., Lee, J.D., Lowe, A., McGovern, A., Przybylo, V., Radford, J.T., Roth, E., Sutter, C., Tissot, P., Roebber, P., Stewart, J.Q., White, M., Williams, J.K., 2023. Trust and trustworthy artificial intelligence: A research agenda for ai in the environmental sciences. *Risk Analysis* 44, 1498–1530. doi:10.1111/risa.14245.
- Brotzge, J.A., Wang, J., Thorncroft, C.D., Joseph, E., Bain, N., Bassill, N., et al., 2020. A technical overview of the new york state mesonet standard network. *Journal of Atmospheric and Oceanic Technology* 37, 1827–1845. doi:10.1175/JTECH-D-19-0220.1.
- Call, D.A., Flynt, G.A., 2022. The impact of snowfall on crashes, traffic volume, and revenue on the new york state thruway. *Weather and Climate and Society* 14, 131–141. doi:10.1175/WCAS-D-21-0074.1.
- Carrillo, J., Crowley, M., 2020. Integration of roadside camera images and weather data for monitoring winter road surface conditions. doi:10.48550/arXiv.2009.12165. arXiv preprint.
- Carrillo, J., Crowley, M., Pan, G., Fu, L., 2020. Design of efficient deep learning models for determining road surface condition from roadside camera images and weather data. doi:10.48550/arXiv.2009.10282. arXiv preprint.

- Chang, J., Walker, C., 2022. Correlating machine learning classification of traffic camera images with snow-related vehicular crashes in new york state. UK Scientific Publishing Limited Prevention and Treatment of Natural Disasters (PTND) 1. doi:10.54963/ptnd.v1i12.65.
- Chase, R.J., Harrison, D.R., Lackmann, G.M., McGovern, A., 2023. A machine learning tutorial for operational meteorology. part ii: Neural networks and deep learning. *Weather and Forecasting* 38, 1271–1293. doi:10.1175/WAF-D-22-0187.1.
- Chollet, F., 2017. Xception: Deep learning with depthwise separable convolutions. doi:10.1109/CVPR.2017.195. arXiv preprint.
- Chollet, F., et al., 2015. Keras. open-source library. URL: <https://keras.io>. [Online] Available: <https://keras.io>. Accessed on: March 23, 2022.
- Coe, K., Scacco, J.M., 2017. Content Analysis, Quantitative. Wiley. chapter n/a. pp. 1–11. doi:10.1002/9781118901731.iecrm0045.
- Deng, J., Dong, W., Socher, R., Li, L.J., Li, K., Fei-Fei, L., 2009. Imagenet: A large-scale hierarchical image database, in: 2009 IEEE Conference on Computer Vision and Pattern Recognition, Miami, FL, USA. pp. 248–255. doi:10.1109/CVPR.2009.5206848.
- FHA, 2023. How do weather events impact roads. U.S. Department of Transportation, Federal Highway Administration. Available at: <https://ops.fhwa.dot.gov/weather/index.asp>. Accessed on: 21 March 2024.
- Google, 2024. Teachable machine. <https://teachablemachine.withgoogle.com/>. Accessed 29 May 2025.
- Géron, A., 2020. Hands-On Machine Learning with Scikit-Learn, Keras, and TensorFlow. 2nd ed., O'Reilly Media, Sebastopol, CA, USA.
- He, K., Zhang, X., Ren, S., Sun, J., 2015. Deep residual learning for image recognition. doi:10.48550/arXiv.1512.03385. arXiv preprint.
- Hollance, M., 2022. Reliability diagrams. GitHub Repository. URL: <https://github.com/hollance/reliability-diagrams>. accessed 19 October 2022.
- Howard, A.G., Zhu, M., Chen, B., Kalenichenko, D., Wang, W., Weyand, T., et al., 2017. Mobilenets: Efficient convolutional neural networks for mobile vision applications. doi:10.48550/arXiv.1704.04861. arXiv preprint.
- HRRR, 2024. High-resolution rapid refresh (hrrr) model. National Oceanic & Atmospheric Administration. Available at: <https://rapidrefresh.noaa.gov/hrrr/>. Accessed 10 February 2024.
- Huang, G., Liu, Z., Van Der Maaten, L., Weinberger, K.Q., 2016. Densely connected convolutional networks. doi:10.48550/arXiv.1608.06993. arXiv preprint.
- Huang, S., Tan, Q., Fan, Q., Zhang, Z., Zhang, Y., Li, X., 2024. Nighttime agglomerate fog event detection considering car light glare based on video. *International Journal of Transportation Science and Technology* doi:10.1016/j.ijstst.2024.08.006.
- Jiang, X., Osl, M., Kim, J., Ohno-Machado, L., 2011. Smooth isotonic regression: A new method to calibrate predictive models, in: AMIA Joint Summits on Translational Science Proceedings, pp. 16–20.
- Jonsson, P., 2011. Classification of road conditions: From camera images and weather data, in: 2011 IEEE International Conference on Computational Intelligence for Measurement Systems and Applications (CIMSAs) Proceedings, Ottawa, ON, Canada. pp. 1–6. doi:10.1109/CIMSAs.2011.6059917.
- Kawai, S., Takeuchi, K., Shibata, K., Horita, Y., 2014. A smart method to distinguish road surface conditions at night-time using a car-mounted camera. *IEEJ Transactions on Electronics, Information and Systems* 134, 878–884. doi:10.1541/iej.134.878.
- Kawarabuki, H., Onoguchi, K., 2014. Snowfall detection under bad visibility scene, in: 17th International IEEE Conference on Intelligent Transportation Systems (ITSC), Qingdao, China. pp. 3058–3063. doi:10.1109/ITSC.2014.6958181.
- Khan, M.N., Ahmed, M.M., 2022. Weather and surface condition detection based on road-side webcams: Application of pre-trained convolutional neural network. *International Journal of Transportation Science and Technology* 11, 468–483. doi:10.1016/j.ijstst.2021.06.003.
- Lee, J., Hong, B., Shin, Y., Jang, Y.J., 2016. Extraction of weather information on road using cctv video, in: 2016 International Conference on Big Data and Smart Computing (BigComp), Hong Kong, China. pp. 529–531. doi:10.1109/BIGCOMP.2016.7425986.
- Liu, B., Li, C., Shi, B., Deng, R., 2025. Hct- lstm: Integrating habit, current situation, and tendency for driving safety state prediction in adverse weather conditions. *International Journal of Transportation Science and Technology* doi:10.1016/j.ijstst.2025.04.005.
- NYS DOT, 2025. 511ny: Real-time traffic and travel information. New York State Department of Transportation. URL: <https://511ny.org>. accessed: 26, January 2022.
- Omer, R., Fu, L., 2010. An automatic image recognition system for winter road surface condition classification, in: 13th International IEEE Conference on Intelligent Transportation Systems, Funchal, Portugal. pp. 1375–1379. doi:10.1109/ITSC.2010.5625290.
- Pan, G., Fu, L., Yu, R., Muresan, M., 2018. Winter road surface condition recognition using a pretrained deep convolutional network. doi:10.48550/arXiv.1812.06858. arXiv preprint.
- Park, D., Park, N., Lee, S., Park, J., Kim, D., 2024. Hierarchical dynamic modeling for highway network real-time risk forecasting with digitalized vehicle data. *International Journal of Transportation Science and Technology* doi:10.1016/j.ijstst.20

24.10.011.

- Pedregosa, F., Varoquaux, G., Gramfort, A., Michel, V., Thirion, B., Grisel, O., et al., 2011. Scikit-learn: Machine learning in python. *Journal of Machine Learning Research* 12, 2825–2830.
- Qian, Y., Almazan, E.J., Elder, J.H., 2016. Evaluating features and classifiers for road weather condition analysis, in: 2016 IEEE International Conference on Image Processing (ICIP), Phoenix, AZ, USA. pp. 4403–4407. doi:10.1109/ICIP.2016.7533192.
- Rothemberger, J.C., Diochnos, D.I., 2024. Meta co-training: Two views are better than one. doi:10.48550/arXiv.2311.18083. arXiv preprint.
- Simonyan, K., Zisserman, A., 2015. Very deep convolutional networks for large-scale image recognition. doi:10.48550/arXiv.1409.1556. arXiv preprint.
- Sirirattapanol, C., Nagai, M., Witayangkurn, A., Pravinvongvuth, S., Ekpanyapong, M., 2019. Bangkok cctv image through a road environment extraction system using multi-label convolutional neural network classification. *ISPRS International Journal of Geo-Information* 8, 128. doi:10.3390/ijgi8030128.
- Sun, Z., Jia, K., 2013. Road surface condition classification based on color and texture information, in: 2013 Ninth International Conference on Intelligent Information Hiding and Multimedia Signal Processing, Beijing, China. pp. 137–140. doi:10.1109/IIH-MSP.2013.43.
- Sutter, C., Sulia, K., Bassill, N.P., Thorncroft, C.D., Wirz, C.D., Przybylo, V., Cains, M.G., Radford, J., Evans, D.A., 2025a. Quantitative content analysis data for hand labeling road surface conditions in new york state department of transportation camera images. Zenodo doi:10.5281/zenodo.15257486.
- Sutter, C., Sulia, K.J., Bassill, N., Wirz, C., Przybylo, V., Cains, M., Radford, J., Evans, A., Thorncroft, C.D., 2025b. Datasheet: Hand-labeled road surface conditions in new york state department of transportation camera images. Zenodo doi:10.5281/zenodo.17080580. [Dataset].
- Szegedy, C., Liu, W., Jia, Y., Sermanet, P., Reed, S., Anguelov, D., et al., 2014. Going deeper with convolutions. doi:10.48550/arXiv.1409.4842. arXiv preprint.
- TensorFlow Developers, 2024. Tensorflow. Zenodo doi:10.5281/zenodo.4724125.
- XCITE, 2025. XCITE Laboratory. Atmospheric Sciences Research Center, University at Albany, State University of New York. Available at: <https://www.albany.edu/asrc/xcite-laboratory>. Accessed on: 1 September 2022.
- Wirz, C.D., Sutter, C., Demuth, J.L., Mayer, K.J., Chapman, W.E., Cains, M.G., et al., 2024. Increasing the reproducibility and replicability of supervised ai/ml in the earth systems science by leveraging social science methods. *Earth and Space Science* 11. doi:10.1029/2023EA003364.
- Wu, M., Kwon, T.J., 2022. An automatic architecture designing approach of convolutional neural networks for road surface conditions image recognition: Tradeoff between accuracy and efficiency. *Journal of Sensors* 2022, 1–11. doi:10.1155/2022/3325282.
- Yamada, M., Ueda, K., Horiba, I., Sugie, N., 2001. Discrimination of the road condition toward understanding of vehicle driving environments. *IEEE Transactions on Intelligent Transportation Systems* 2, 26–31. doi:10.1109/6979.911083.
- Yan, X., Luo, Y., Zheng, X., 2009. Weather recognition based on images captured by vision system in vehicle, in: 6th International Symposium on Neural Networks, Wuhan, China. pp. 390–398. doi:10.1007/978-3-642-01513-7_42.
- Yang, H., Jang, H., Kang, J., Jeong, D., 2014. Classification algorithm for road surface condition. *IJCSNS International Journal of Computer Science and Network Security* 14.
- Zhang, C., Nateghinia, E., Miranda-Moreno, L.F., Sun, L., 2022. Pavement distress detection using convolutional neural network (cnn): A case study in montreal, canada. *International Journal of Transportation Science and Technology* 11, 298–309. URL: <https://www.sciencedirect.com/science/article/pii/S2046043021000307>, doi:<https://doi.org/10.1016/j.ijtst.2021.04.008>.
- Zhang, C., Wang, W., Su, Y., Bai, X., 2012. Discrimination of highway snow condition with video monitor for safe driving environment, in: 2012 5th International Congress on Image and Signal Processing, Chongqing, China. pp. 1241–1244. doi:10.1109/CISP.2012.6469850.